Photoluminescence and Rutherford backscattering spectrometry study of ion-implanted Er^{3+}-doped $LiNbO_3$ planar waveguides

1998 J. Phys.: Condens. Matter 10 3275

(http://iopscience.iop.org/0953-8984/10/14/016)

J. Phys.: Condens. Matter **10** (1998) 3275–3283. Printed in the UK PII: S0953-8984(98)89068-1

Photoluminescence and Rutherford backscattering spectrometry study of ion-implanted Er^{3+}-doped $LiNbO_3$ planar waveguides

B Herreros†, G Lifante†, F Cussó†, J A Sanz†, A Kling‡, J C Soares‡, M F da Silva§, P D Townsend‖ and P J Chandler‖

† Departamento de Física de Materiales, C-IV, Universidad Autónoma de Madrid, 28049 Madrid, Spain

‡ Centro de Física Nuclear da Universidade de Lisboa, 1699 Lisboa Codex, Portugal

§ Departamento de Física, ITN, 2685 Sacavém, Portugal

‖ Department of Chemistry, Physics and Environmental Science, University of Sussex, Brighton BN1 9QJ, UK

Received 7 November 1997

Abstract. In this work we present a study of Er^{3+}-doped $LiNbO_3$ ion-implanted planar waveguides by laser spectroscopy and Rutherford backscattering spectrometry (RBS). RBS measurements for both random and channelling conditions were carried out in order to investigate the crystal quality of the original crystals and their respective waveguides. The angular dependences of the Nb and Er yields were compared and a non-substitutional fraction of Er^{3+} ions was found in both the bulk crystal and the waveguide. Some deterioration of the crystal quality in the waveguide compared to that in the bulk was also detected. Laser spectroscopy was used to obtain information about the optical properties of the Er^{3+} ions within the waveguides and to compare them with the properties of the Er^{3+} ions in the bulk. The results obtained show that the spectroscopic properties of the waveguide Er^{3+} ions are essentially the same as those of the Er^{3+} ions in the bulk, except a slight broadening of the bands and some changes in the relative intensities.

1. Introduction

Lithium niobate offers a great variety of potential applications in the field of integrated optics since it exhibits very important non-linear properties, such as high electro- and acousto-optic coefficients, and also offers the possibility of doping it with optically active ions to obtain laser action. Moreover, the use of a waveguide configuration increases the efficiency of non-linear processes and the laser gain due to the strong power confinement [1–6]. Among the different laser dopants, the erbium ion is especially useful because its 1.55 μm emission corresponds to one of the low-loss optical windows, and its absorption bands at around 800 and 970 nm are compatible with laser diode pumping.

During the last few years, the optical characterization of $LiNbO_3$:Er^{3+} has attracted considerable interest, and several investigations [7–15] devoted to the spectroscopic study of Er^{3+} ions in $LiNbO_3$ have been published. In addition, recently the utility of Er^{3+}-doped $LiNbO_3$ as a waveguide laser material has been demonstrated, and several active devices [16–20] based on this combination have been reported.

Although the most popular methods for producing waveguides in $LiNbO_3$ (metal in-diffusion [21, 22], proton exchange [23] and ion implantation [24]) are based on a change

0953-8984/98/143275+09$19.50

in the refractive index of the substrate induced by modification of its structure, little attention has been focused on the effects that such changes in the material might have on the spectroscopic properties of the rare-earth ions in the waveguides.

In this work we present a study of Er^{3+}-doped $LiNbO_3$ planar waveguides, with different Er^{3+} doping levels, fabricated by the ion-implantation technique [25]. In order to determine the degree of crystallinity of the waveguides after the ion implantation, the Rutherford backscattering spectrometry (RBS) technique for both random and channelling geometries was used. Furthermore, we also carried out photoluminescence measurements to obtain information about the optical properties of the Er^{3+} ions within the waveguide and their possible changes with respect to those of the ions in the original substrate.

2. Experimental procedure

The Er^{3+}-doped $LiNbO_3$ crystals used for this work were grown at the Autónoma University (Madrid) by the Czochralski technique from grade I Johnson–Matthey powders. These crystals were doped with Er_2O_3 and MgO which were added to the congruent melt at different doping levels. One crystal was singly doped with 0.2 mol% of Er^{3+} in the melt, another one with 0.5 mol% Er^{3+} and 6 mol% MgO and a third one with 1 mol% Er^{3+} and 5 mol% MgO, all of the percentages being referred to that of Nb^{5+}. From each crystal a rectangular sample was cut perpendicular to the *c*-axis and carefully polished.

Each of the substrates was implanted at the Van de Graaff accelerator of Sussex University with He^+ ions of 2 MeV to define planar optical waveguides on one of its surfaces. The ion dose was 2×10^{16} ions cm^{-2} with an average beam current of 1 μA cm^{-2}. From the value of the He^+-beam energy used for the implantation, the depth of the waveguides can be estimated [26] to be of the order of 4 μm. The samples were held at a temperature of 77 K during the implantation to ensure an efficient retention of damage. After the ion implantation the samples were annealed in air at a temperature of 250 °C for 30 min to remove colour centres formed during the implantation process. Subsequently, the ends of the waveguides were carefully polished to allow end-fire coupling of light.

The luminescence measurements were accomplished by using an Ar-ion laser (λ = 488.0 nm) as an excitation source. The experimental set-up employed to carry out the emission measurements in the waveguide at room and low temperature has been described elsewhere [27]. The emissions were detected by means of a silicon detector (Telefunken BPW-34) and a photomultiplier tube (EMI QB558), according to the spectral range.

The RBS/channelling experiments were performed at the 3.1 MeV Van de Graaff accelerator of Instituto Tecnológico e Nuclear at Sacavém (Portugal). A He^+ beam of 1.6 MeV was used, the typical He^+-beam current being below 1 nA, in order to minimize radiation damage and electronic pile-up. The samples were mounted on a two-axis goniometer which allowed two rotations, and the backscattered He^+ particles were detected with two surface barrier detectors at 140° and 180° relative to the beam direction, the latter being an annular detector. For the initial energy of the incident beam, the accessible depth is limited to about 2 μm, which is smaller than the total waveguide thickness. Thus it is ensured that the waveguide signal only carries information about the waveguide.

3. Results

Figure 1 shows several emission spectra for the bulk (continuous line) and the ion-implanted waveguide (dotted line) of the $LiNbO_3$:0.2% Er^{3+} sample corresponding to different Er^{3+}

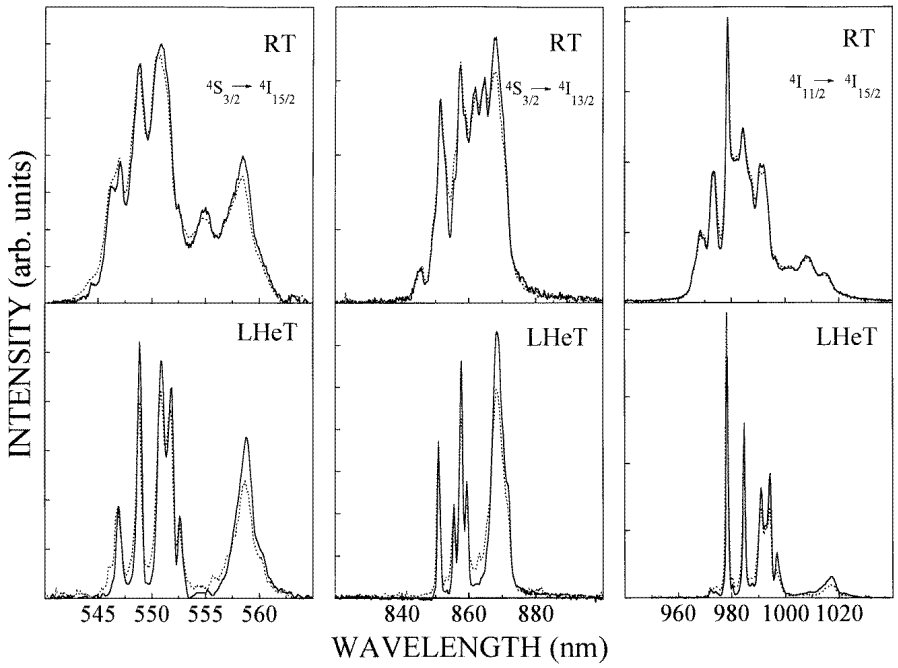

Figure 1. σ-polarized emission spectra at RT and LHeT (upper and lower part, respectively), under $\lambda = 488.0$ nm excitation, for the bulk (continuous line) and the ion-implanted waveguide (dotted line) of the $LiNbO_3$:0.2% Er^{3+} sample corresponding to the transitions $^4S_{3/2} \rightarrow {}^4I_{15/2}$ ($\approx$550 nm), $^4S_{3/2} \rightarrow {}^4I_{13/2}$ ($\approx$860 nm) and $^4I_{11/2} \rightarrow {}^4I_{15/2}$ ($\approx$980 nm).

transitions. The upper part of figure 1 shows the spectra at room temperature, whilst the lower part displays the same emissions at low temperature. In order to compare waveguide emissions to those of bulk, it is advisable to use polarized emissions to avoid the effect of possible differences in losses for the TE and TM polarizations inside the waveguide. This ion-implanted waveguide exhibited lower losses for TE than for TM and, hence, σ-polarized emissions had a better signal-to-noise ratio; that is why the study has concentrated on σ-polarized spectra. The spectra are normalized to the same area under the curve for display purposes.

The Ar^+-laser excitation at $\lambda = 488.0$ nm populates the state $^4F_{7/2}$ of Er^{3+} ions (see figure 2 for a partial energy level diagram) from which a rapid non-radiative de-excitation down to the $^4S_{3/2}$ state takes place. Among the different emissions that can be observed from this state, the $^4S_{3/2} \rightarrow {}^4I_{15/2}$ ($\approx$550 nm) and the $^4S_{3/2} \rightarrow {}^4I_{13/2}$ ($\approx$860 nm) transitions are the most intense ones, their branching ratios being 70% [12] and 25% [12], respectively. The $^4I_{11/2}$ state is also populated, mostly from non-radiative paths, and from this state the $^4I_{11/2} \rightarrow {}^4I_{15/2}$ ($\approx$980 nm) transition can be detected.

When comparing the bulk and waveguide spectra of figure 1, it is difficult to see any change at room temperature due to the large band widths, but by inspecting the spectra at LHeT it can be appreciated that there is a slight broadening of the bands for the waveguide together with some changes in the relative intensities. All of the waveguide spectra show essentially the same structure as for the bulk, and both types are consistent with the reported [28, 29] incorporation of Er^{3+} into the Li^+ octahedron showing C_3 symmetry. The polarization characters of the bands are also preserved in the waveguide and are also

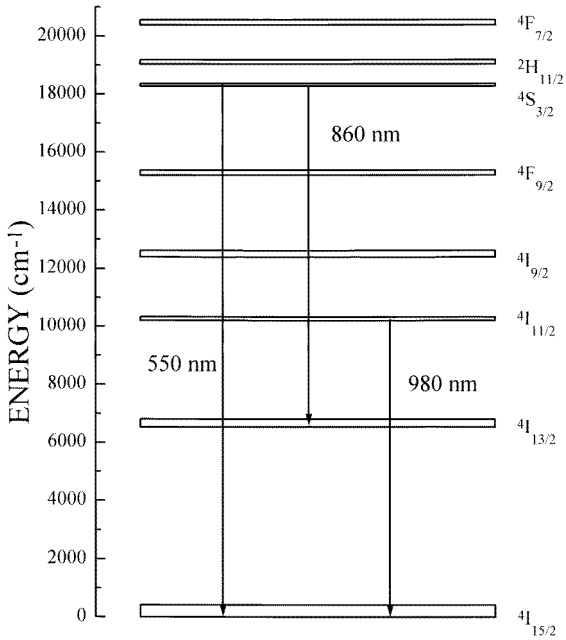

Figure 2. A partial energy level diagram for Er^{3+} ions in $LiNbO_3$.

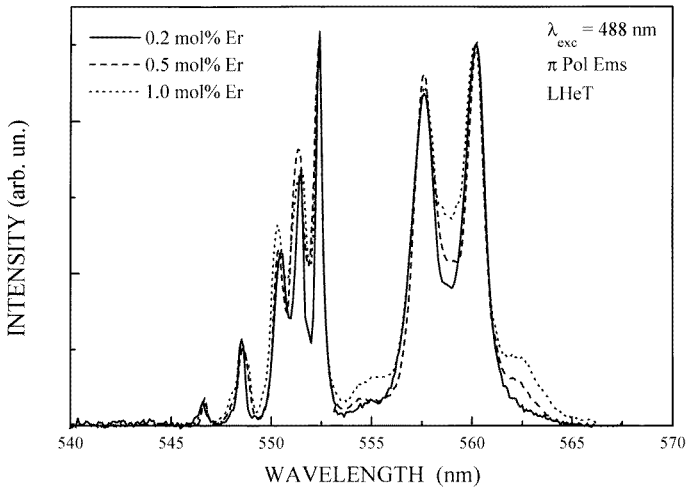

Figure 3. LHeT π-polarized emission spectra, under $\lambda = 488.0$ nm excitation, for the bulk of samples $LiNbO_3$:0.2% Er^{3+} (continuous line), $LiNbO_3$:MgO:0.5% Er^{3+} (broken line) and $LiNbO_3$:MgO:1% Er^{3+} (dotted line) corresponding to the $^4S_{3/2} \rightarrow {}^4I_{15/2}$ transition.

consistent with the selection rules for C_3 symmetry.

As regards the observed spectrum broadening, it was detected that in bulk crystals there also exists a broadening of the bands with increasing Er^{3+} concentration prior to ion implantation. This can be observed in figure 3, where a comparison of the $^4S_{3/2} \rightarrow {}^4I_{15/2}$ π-polarized emission spectra at LHeT for the bulk crystals of the samples under study is

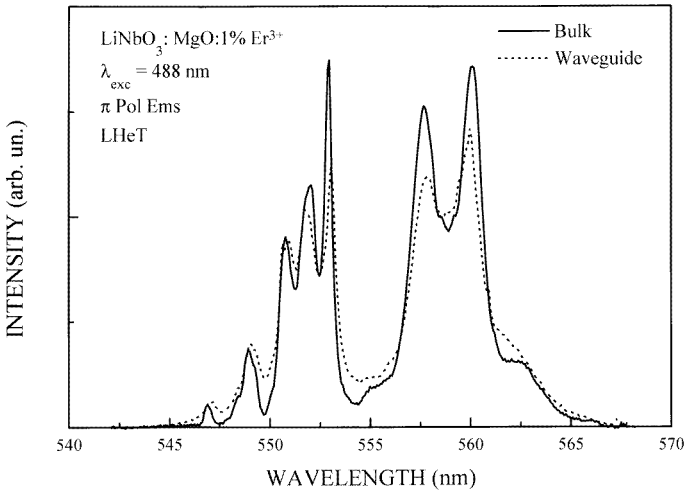

Figure 4. LHeT π-polarized emission spectra, under $\lambda = 488.0$ nm excitation, for the bulk (continuous line) and the ion-implanted waveguide (dotted line) of the $LiNbO_3$:MgO:1% Er^{3+} sample corresponding to the $^4S_{3/2} \rightarrow {}^4I_{15/2}$ transition.

presented. For the waveguide luminescence, figure 4 shows the same emission spectra for the bulk (continuous line) and the ion-implanted waveguide (dotted line) of the $LiNbO_3$:MgO:1.0% Er^{3+} sample. When comparing the waveguide spectra to those for the bulk, it was detected that the broadening of the waveguide spectrum increases with increasing Er^{3+} concentration for all of the samples under study.

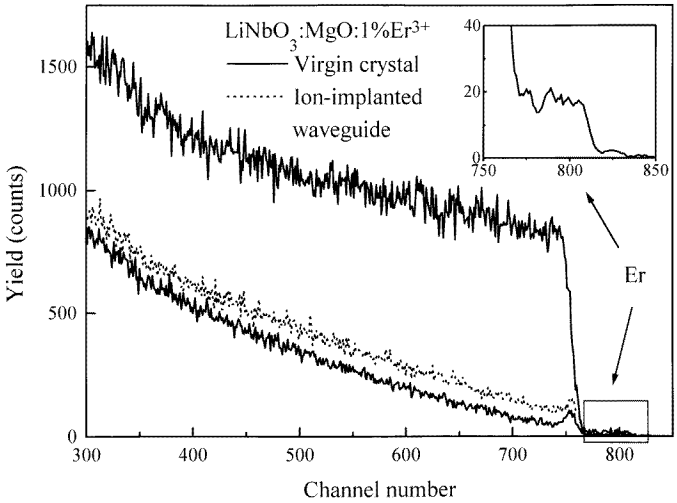

Figure 5. Random and ⟨0001⟩- (*c*-axis-) aligned spectra for the bulk (continuous line) and the waveguide (dotted line) of the $LiNbO_3$:MgO:1% Er^{3+} sample.

In order to study the crystal structure and defect distribution, we have performed RBS measurements on both the bulk and the waveguide of the three samples. Backscattering energy spectra for a beam incident along the ⟨0001⟩ crystallographic axis (*c*-axis) are

shown in figure 5 for the bulk (continuous line) and the waveguide (dotted line) of the $LiNbO_3$:MgO:1.0% Er^{3+} sample. Also included is the random (non-channelling-direction) spectrum of the virgin crystal (bulk), which was perfectly coincident, within the noise scatter, with the random spectrum for the waveguide. The ⟨0001⟩ axis for the waveguide was found to be the same direction as for the substrate, indicating that the ion implantation has preserved the crystallographic orientation in the waveguide.

As can be seen in figure 5, the aligned spectra of the bulk and the waveguide are quite similar, although it can be observed that the aligned yield for the waveguide is higher than that for the bulk. In fact, the minimum yield, χ_{min}, defined here as the ratio of the Nb average yield in the depth region from the surface to 1500 Å (excluding the surface peak) of the aligned and the random spectrum, was found to be 7% for the virgin crystal and 13% for the waveguide, indicating that the crystal quality of the ion-implanted waveguide is lower than that of the virgin crystal.

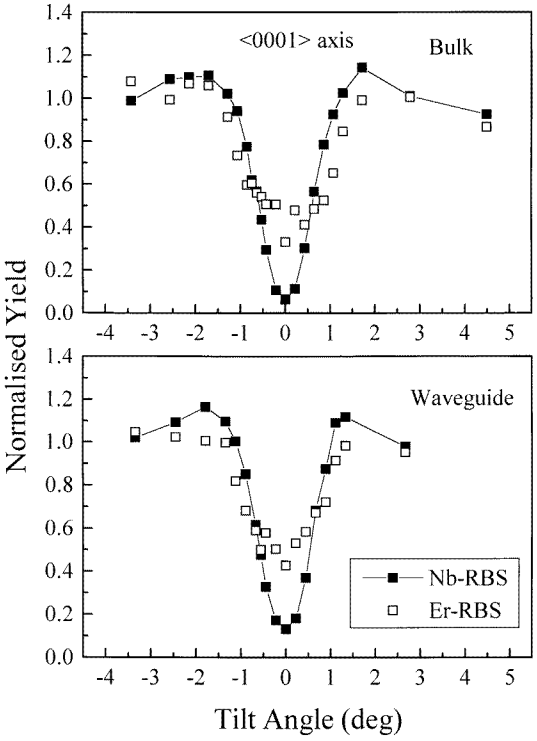

Figure 6. The angular dependence along the ⟨0001⟩ axis of the normalized backscattering yield of 1.6 MeV He^+ ions from Nb and Er for the bulk (upper part) and ion-implanted waveguide (lower part) of the $LiNbO_3$:MgO:1% Er^{3+} sample.

Since Er has a higher mass than Nb, the backscattering signals due to niobium and erbium can be well separated from each other (see the inset in figure 5) and can be evaluated separately. The angular dependences of the normalized yield for Nb and Er corresponding to the ⟨0001⟩ axis for the $LiNbO_3$:MgO:1% Er^{3+} sample are depicted in figure 6. The upper part of figure 6 corresponds to the bulk, and the lower part to the waveguide. These angular scans were obtained by monitoring the scattering yields of Er and Nb over two windows that are narrow and very near the surface (excluding the surface peak) in the

backscattering spectrum, which correspond to the same depth within the sample. The yields were normalized to the integrated random value over the same window and plotted as a function of the angle between the beam direction and the axis.

As regards the Nb angular scans of figure 6 (full symbols), no changes either in shape or in width are observed when comparing the waveguide and the bulk, the only difference being a higher value of the Nb minimum yield for the waveguide. As regards the Er signal, supposing that all of the Er ions in the crystal were located along the Li–Nb strings parallel to the *c*-axis, the Er angular scan should be almost identical, both in magnitude and in width, to that for Nb. The angular scans in figure 6 show that the Er signal follows that of Nb but with a significantly higher minimum yield, indicating that, besides a fraction of Er ions aligned along the *c*-axis, there is also another fraction of Er ions present, which occupies random positions or is forming precipitates, which show no angular dependence in the yield curve (random fraction). This is in agreement with previous work [30] where Er ions were found to occupy displaced Li sites together with a random fraction, in contrast to other rare-earth ions which have been reported to occupy displaced Li sites without the presence of any random fraction for a similar concentration range.

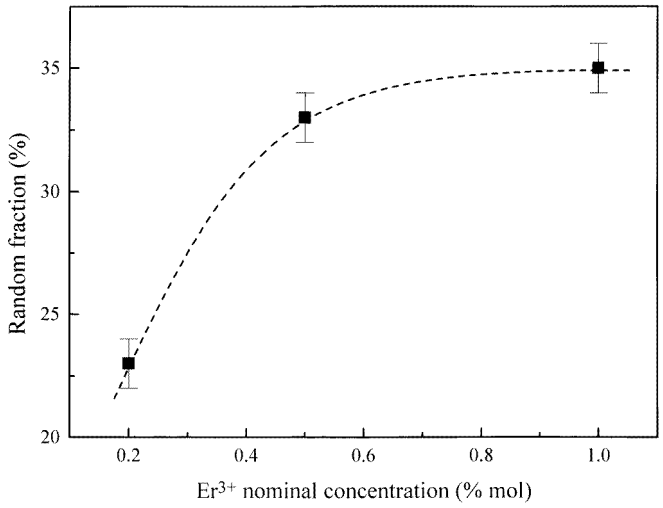

Figure 7. The Er^{3+} concentration dependence of the Er^{3+} random fraction for the samples studied.

For the other two samples, a random fraction of Er^{3+} ions was also detected, which was always comparable for the bulk and the waveguide of each sample. These results are presented in figure 7 where it can be observed that such a random fraction increases in size with increasing Er^{3+} concentration.

4. Discussion

Ion-implanted waveguides are expected to preserve most of the properties of the original host since the guiding layer corresponds to the region confined between air and the nuclear damage region, and it has only suffered from the electronic damage that leads to the appearance of colour centres, which are easily removed by annealing.

This behaviour is confirmed by the optical data that we have obtained, showing that the

spectroscopic properties of Er^{3+} are mostly preserved in the waveguide. The broadening of the emission bands is not very important, and the fact that the number of bands and the polarization characters are preserved indicates that the symmetry of the local environment of the optically active Er^{3+} ions in the bulk and the waveguide is maintained.

As regards the RBS data, they show that the ion-implantation process has had a deleterious effect on the properties of the virgin crystal in the guiding region, since the change of χ_{min} from 7% (bulk) to 13% (waveguide) is significant and cannot be simply due to electronic damage. In contrast, preliminary studies [31, 32] performed on Nd^{3+}-doped and Tm^{3+}-doped $LiNbO_3$ ion-implanted waveguides fabricated under similar conditions have shown that the crystal quality was not altered by the ion implantation and no random fraction was detected for these two ions.

No significant changes can be noticed between the Er angular scan of the bulk and that of the waveguide, and in both cases an increase of the size of the Er random fraction with increasing Er concentration is observed, pointing to the possible existence of some kind of precipitate or cluster both in the bulk and in the waveguide. On the other hand, the relative broadening of the waveguide emission spectra with respect to the bulk ones increases with increasing Er^{3+} concentration. Therefore, we would suggest that the non-substitutional fraction of Er^{3+} ions in $LiNbO_3$ favours damage production during the waveguide formation process, either during ion implantation or during the subsequent annealing.

In conclusion, we have shown by means of two different techniques, optical spectroscopy and RBS/channelling, how the structural properties of Er^{3+}-doped $LiNbO_3$ are mostly preserved after He^+-ion implantation at a dose of 2×10^{16} ions cm^{-2} and at an energy of 2 MeV, suggesting ion implantation as a good method for fabricating waveguide lasers in Er^{3+}-doped $LiNbO_3$.

Acknowledgments

This work was partially supported by the Comisión Interministerial de Ciencia y Tecnología (CICYT, Spain, Project No TIC95-0166) and the Acción Integrada Hispano-Británica 162-B. B Herreros holds a grant of the Ministerio de Educación y Ciencia and P J Chandler is supported by the Optical Research Centre at Southampton University.

References

[1] Field S J, Hanna D C, Shepherd D P, Tropper A C, Chandler P J, Townsend P D and Zhang L 1991 Ion-implanted Nd:MgO:$LiNbO_3$ planar waveguide laser *Opt. Lett.* **16** 481

[2] Amin J, Hempstead M, Román J E and Wilkinson J S 1994 Tunable coupled-cavity waveguide laser at room temperature in Nd-diffused Ti:$LiNbO_3$ *Opt. Lett.* **19** 1541

[3] Jones J K, de Sandro J P, Hempstead M, Shepherd D P, Large A C, Tropper A C and Wilkinson J S 1995 Channel waveguide laser at 1 μm in Yb-indiffused $LiNbO_3$ *Opt. Lett.* **20** 1477

[4] de Sandro J P, Jones J K, Shepherd D P, Hempstead M, Wang J and Tropper A C 1996 Non-photorefractive CW Tm-indiffused Ti:$LiNbO_3$ waveguide laser operating at room temperature *IEEE Photon. Technol. Lett.* **8** 209

[5] Lalier E, Pochole J P, Papuchon M, He Q, De Micheli M P and Ostrowsky D B 1992 Integrated Q-switched Nd:MgO:$LiNbO_3$ waveguide laser *Electron. Lett.* **28** 1428

[6] Brinkmann R, Sohler W, Suche H and Wersig C 1992 Fluorescence and laser operation in single-mode Ti-diffused Nd:MgO:$LiNbO_3$ waveguide structures *J. Quantum Electron.* **28** 466

[7] Gabrielyan V T, Kaminskii A A and Li L 1970 Absorption and luminescence spectra and energy levels of Nd^{3+} and Er^{3+} ions in $LiNbO_3$ crystals *Phys. Status Solidi* a **3** K37

[8] Polgar K and Skvortsov A P 1985 Stark effect in f–f spectra of $LiNbO_3$:Er^{3+} *Opt. Spectrosc.* **58** 140

[9] Duchowicz R, Núñez L, Tocho J O and Cussó F 1993 MgO-induced effects on the optical properties of Er-doped $LiNbO_3$ *Solid State Commun.* **88** 439
[10] Tsuboi T, Ruan Y F and Adachi G 1995 Green luminescence from Er^{3+} ions in $LiNbO_3$ crystals *Phys. Status Solidi* b **187** K75
[11] Milori D M B P, Moraes I J, Hernandes A C, de Souza R R, Li M Siu and Terrile M C 1995 Optical and ESR study of Er^{3+} in $LiNbO_3$ *Phys. Rev.* B **51** 3206
[12] Núñez L, Lifante G and Cussó F 1996 Polarization effects on the line-strength calculations of Er^{3+}-doped $LiNbO_3$ *Appl. Phys.* B **62** 485
[13] Gill D M, Wright J C and McCaughan L 1994 Site characterization of rare-earth-doped $LiNbO_3$ using total site selective spectroscopy *Appl. Phys. Lett.* **64** 2483
[14] Witte O, Stolz H and von der Osten W 1996 Upconversion and site-selective spectroscopy in erbium-doped $LiNbO_3$ *J. Phys. D: Appl. Phys.* **29** 561
[15] Gill D M, McCaughan L and Wright J C 1996 Spectroscopic site determinations in erbium-doped lithium niobate *Phys. Rev.* B **53** 2334
[16] Brinkmann R, Sohler W and Suche H 1991 Continuous-wave erbium diffused $LiNbO_3$ waveguide laser *Electron. Lett.* **27** 415
[17] Becker P, Brinkmann R, Dinand M, Sohler W and Suche H 1992 Er-diffused Ti:$LiNbO_3$ waveguide laser of 1563 and 1576 nm emission wavelengths *Appl. Phys. Lett.* **61** 1257
[18] Suche H, Baumann I, Hiller D and Sohler W 1993 Mode-locked Er:Ti:$LiNbO_3$ waveguide laser *Electron. Lett.* **29** 1111
[19] Suche H, Wessel R, Westenhöfer S and Sohler W 1995 Harmonically mode-locked Ti:Er:$LiNbO_3$ waveguide laser *Opt. Lett.* **20** 596
[20] Söchtig J, Groß R, Baumann I, Sohler W, Schütz H and Widner R 1995 DBR waveguide laser in erbium-diffusion-doped $LiNbO_3$ *Electron. Lett.* **31** 551
[21] Schmidt R V and Kaminow I P 1974 Metal-diffused optical waveguides in $LiNbO_3$ *Appl. Phys. Lett.* **25** 458
[22] Herreros B and Lifante G 1995 $LiNbO_3$ optical waveguides by Zn diffusion from vapor phase *Appl. Phys. Lett.* **66** 1449
[23] De Micheli M P, Ostrowsky D B, Korkishko Y N and Bassi P 1995 Proton exchange waveguides in $LiNbO_3$ and in $LiTaO_3$: structural and optical properties *Insulating Materials for Optoelectronics: New Developments* ed F Agulló-López (London: World Scientific) ch 12
[24] Townsend P D 1986 Ion implantation—an introduction *Contemp. Phys.* **27** 241
[25] Chandler P J, Zhang L and Townsend P D 1990 Ion implanted waveguides in doped $LiNbO_3$ *Electron. Lett.* **26** 332
[26] Townsend P D, Chandler P J and Zhang L 1994 *Optical Effects of Ion Implantation* (Cambridge: Cambridge University Press)
[27] Herreros B, Lifante G, Cussó F, Townsend P D and Chandler P J 1995 Luminescence spectroscopy of Nd^{3+} in ion-implanted $LiNbO_3$:Nd:MgO planar waveguides *J. Phys. D: Appl. Phys.* **28** 1687
[28] Gog Th, Griebenow M and Materlik G 1993 X-ray standing wave determination of the lattice location of Er diffused into $LiNbO_3$ *Phys. Lett.* **181A** 417
[29] Lorenzo A, Jaffrezic H, Roux B and Boulon G 1995 Lattice location of rare-earth ions in $LiNbO_3$ *Appl. Phys. Lett.* **25** 3735
[30] Rebouta L 1992 Localizaçao de dopantes e caracterizaçao de defeitos em niobato de litio *PhD Thesis* Universidade de Lisboa
[31] Herreros B, Lifante G, Cussó F, Kling A, Soares J C, da Silva M F, Townsend P D and Chandler P J 1995 Structural and optical properties of rare-earth doped lithium niobate waveguides formed by MeV helium implantation *Proc. Symp. on Ion–Solid Interactions for Materials Modification and Processing; 1995 MRS Meeting* vol 396, ed D B Poker *et al* (Pittsburgh, PA: Materials Research Society)
[32] Herreros B, Lifante G, Kling A, Soares J C, da Silva M F, Townsend P D, Chandler P J, Olivares J and Cabrera J M 1996 RBS/channelling study of ion-implanted and proton exchanged $LiNbO_3$:Nd^{3+}:MgO planar waveguides *Opt. Mater.* **6** 281